Int. J. Heat Mass Transfer. Vol. 18, pp. 961–973. Pergamon Press 1975. Printed in Great Britain

INVESTIGATIONS OF THE FACTORS AFFECTING THE PERFORMANCE OF A ROTATING HEAT PIPE

T. C. DANIELS* and F. K. AL-JUMAILY†
Mechanical Engineering Department, University College, Swansea SA2 8PP

(*Received* 12 *September* 1974 *and in revised form* 13 *November* 1974)

Abstract—The rotating heat pipe is a device which utilises a two-phase heat-transfer cycle. Rotation about the longitudinal axis generates a centrifugal force field and a component of this acting along the tapered wall pumps the condensate back to the evaporator.

A theoretical Nusselt type analysis is proposed for the condensate film taking into account the drag effects of contra-flowing vapour. A performance prediction relates rates of heat transfer, rotational speeds, temperature differences across condensate films, fluid properties and heat pipe geometry.

Experimental investigation tests the analysis with good agreement for the two Arcton 113 and 21 fluids but no agreement with water. An explanation for this is proposed.

NOMENCLATURE

- Ac, cross-section area at entrance to the condenser;
- Cp, specific heat at constant pressure;
- f, friction factor;
- F, force;
- g, gravitation acceleration;
- h_{fg}, latent heat of vaporization;
- $h_{\bar{f}g}$, $h_{fg}+0{\cdot}35\,Cp\,\theta s$;
- h, average condensation heat-transfer coefficient;
- h_x, local condensation heat-transfer coefficient;
- L, length of condenser section;
- $\dot{m}v$, mass flow rate of vapour;
- m, mass flow rate of condensate at section x for unit periphery;
- m_L, mass flow rate of condensate at $x = L$ per unit periphery;
- P, pressure;
- P_v, vapour pressure;
- Q, heat-transfer rate;
- Qx, local heat flux;
- r, average condenser radius;
- ts, saturation temperature;
- tw, condenser wall temperature;
- u_v, vapour velocity;
- u, liquid condensate velocity;
- u_δ, liquid condensate velocity of $y = \delta$;
- Um, mean liquid condensate velocity;
- x, position co-ordinate;
- y, position co-ordinate;
- Z, characteristic dimension of the liquid–vapour interface.

Greek symbols

- α, taper angle;
- ρ, liquid density;
- ρ_v, vapour density;
- μ, liquid dynamic viscosity;
- μ_v, vapour dynamic viscosity;
- δ, condensate layer thickness;
- τ, shear stress;
- τ_v, shear stress of liquid vapour interface;
- θs, temperature difference $(ts - tw)$;
- ω, angular velocity.

Dimensionless groups

- Sh, Sherwood number;
- Dr, friction number;
- Nu, Nusselt number;
- Rev, two-phase Reynolds number;
- Ref, liquid film Reynolds number;
- Red, vapour Reynolds number.

*Senior Lecturer.
†Research Assistant.

INTRODUCTION

THE "HEAT PIPE" was originally patented in 1944 by Gaugler [1] as a self-contained evaporating-condensing device with recycling of the fluid by capillary action. The first paper on heat pipes came in 1964 and was given by Grover *et al.* [2]. Since that time interests has grown to such an extent that whole conferences have been devoted to the subject [3].

A capillary heat pipe is a sealed tube whose inside wall is lined with a porous wick which is saturated with a working liquid. The tube is heated at one end causing the liquid to evaporate and the vapour condenses at the other end giving up its latent heat. In an operating heat pipe there is continuous flow of vapour from evaporator to condenser and the liquid is continuously re-cycled by capillary action in the opposite direction back to the evaporator.

The following references [4–6] give a full report on the construction, limits of operation and characteristics of capillary heat pipes.

The rotating heat pipe is a sealed hollow shaft (see Fig. 1) with a slight internal taper along its axial length and contains a fixed amount of working fluid. Rotating heat pipes are similar to capillary heat pipes in that they

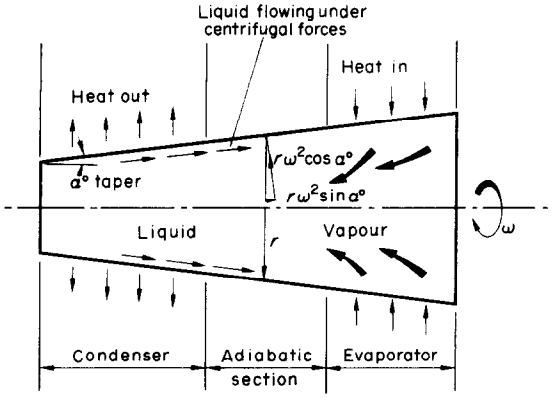

FIG. 1. Schematic diagram of wickless rotating heat pipe.

consist of three longitudinal sections, viz. evaporator, adiabatic and condenser sections. Heat is transferred from an external source through the walls of the evaporator to the working fluid causing evaporation. The vapour flows towards the condenser where it condenses and ultimately transfers its latent heat through the condenser layer and wall to an external cold sink. The adiabatic section separates the evaporator and condenser and provides only a passage for the fluid. Rotation about the longitudinal axis generates a centrifugal force field. A component of this force along the tapered wall pumps the condensate from the smaller diameter condenser section back to the larger diameter evaporator to complete the cycle. Some of the limitations imposed by the failure of a wick capillary structure to provide sufficient pumping force for the continuous return of the condensate to the evaporator are therefore eliminated by the use of the centrifugal force field.

The rotation of the heat pipe has a profound effect on basic heat- and mass-transfer mechanisms involved in its operation. Gray [7] in the first article published on rotating heat pipes arbitrarily divided the heat pipe into the following components: rotating boiler, rotating condenser, two-phase annular flow transfer pipe and a centrifugal pump. Gray *et al.* [8] in their paper on the rotating boiler indicated that high centrifugal acceleration produced smooth, stable inter faces between liquid and vapour during the boiling of water at one atmosphere with heat fluxes up to 257 W/cm^2 and accelerations up to 400 g. Boiling heat transfer coefficients at high accelerations and high heat fluxes are roughly the same as at 1 g; however the burn out or critical heat flux does increase at high accelerations. Costello and Adams [9] obtained a theoretical relation which suggests that critical burn out flux varies with one fourth power of acceleration.

The rotating condenser component maintains a very high condensing coefficient by virtue of the efficient removal of the condensate from the cooler surface by the pumping action. The thermal resistance of the condensate layer is quite small since the high centrifugal force applied causes its thickness to decrease appreciably. This is in contrast to the capillary type heat pipe where a sizeable internal thermal resistance exists due to the internal wicking material and the relatively thick layer of liquid permeating it.

In the adiabatic zone the vapour and liquid flows are transferred counter-currently with the vapour in the centre of the annulus flowing at a much higher velocity than the liquid along the wall.

In 1961 Sparrow and Hartnett [10] carried out a theoretical analysis of a cone rotating in a space filled with vapour at saturation temperature with the condensate forming a laminar film over the cone. A boundary-layer approach was employed with the mass momentum, and energy conservation, as the governing equations. Their similarity solution applied only to cones that are not too slender and in a region sufficiently removed from the apex where the thickness of the boundary layer is constant. Marto *et al.* [11] applied this similarity solution to the inside of a rotating heat pipe condenser section (i.e. a rotating truncated cone) and concluded that their solution had the following two restrictions (a) it only applied to large cone angles (b) the velocity profile of the condensate layer did not satisfy the boundary condition that the velocity must be zero at the beginning of the condenser wall. In an effort to overcome the restrictions Ballback [12] performed a Nusselt [14] type analysis for film condensation on the inside of the rotating truncated cone. He found an expression for the condensate velocity which he could solve by making the following assumptions (a) the condensate film was very thin, (b) the slope of the condensate film was much less than the angle of the truncated cone, and using a boundary condition that the film thickness must be zero at the beginning of the condenser he arrived at a film thickness distribution for the whole condenser. By neglecting the thermal resistance of the condenser wall and outside cooling mechanism Ballback derived an expression for the total heat-transfer rate in the condenser. In later work Daley [13] modified Ballback's analysis to include the thermal resistance of the condenser wall and outside cooling mechanism, this gave heat-transfer rates 37–50% higher than those predicted by Sparrow over a rotational speed range of 800–3200 rev/min. because of the thinner condensate film predicted by Daley. When comparing Ballback's own analysis with Daley the latter gives 10 per cent higher heat-transfer rates. Both Ballback and Daley have in their theoretical work neglected the drag due to vapour friction on the contra flowing condensate film. Neither carried out any experimental investigations to substantiate their theoretical predictions. The following analysis takes into account the drag due to vapour friction and the subsequent experimental work tests this theoretical analysis.

THEORETICAL ANALYSIS OF THE CONDENSATION PROCESS

The heat pipe is in a steady-state condition when the evaporation rate and condensation rate are in equilibrium. Therefore the performance of the heat pipe is strongly related to the efficiency of the condensation process.

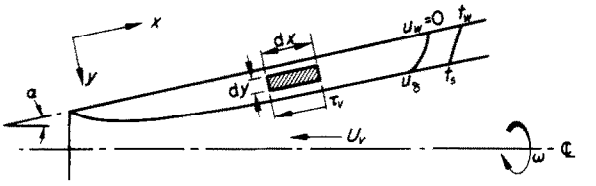

FIG. 2(a). x-Direction forces on the element considered.

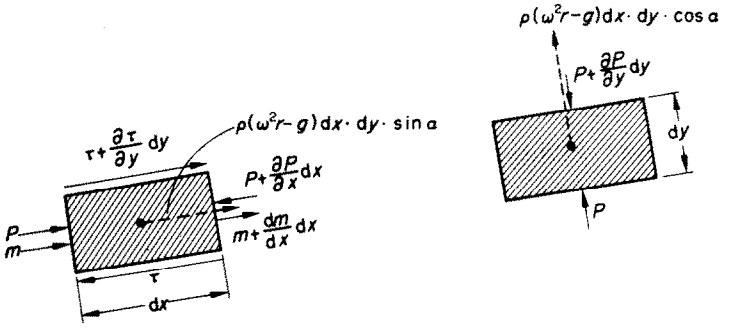

FIG. 2(b). y-Direction forces on the element considered.

FIG. 2. Velocity and temperature distribution in the condensate layer, and coordinate system.

An analysis for laminar filmwise condensation of pure vapour on tubes and plates was first obtained by Nusselt in 1916 [14]. He analysed the case of a continuous film of condensing liquid of increasing thickness flowing down a vertical plate under the effect of gravity. The basic principles of Nusselt's analysis will be followed though some of the conditions are different. (a) the driving force for the condensate is usually centrifugal, (b) the condensation is taking place on the inside surface of the rotating condenser section, (c) the vapour is flowing in the opposite direction to the condensate flow.

When the vapour velocity is high the condensate film is subjected to a drag force which is the result of the vapour friction on the liquid vapour interface and also a momentum drag as the vapour condenses on the slower moving liquid film. Nusselt neglected the effect of these forces while the present analysis takes into account both forms of the drag following the approach of Mayhew *et al.* [15] in their analysis of a vertical stationary condensing section.

In developing the theoretical analysis the following assumptions are made (a) filmwise condensation (b) laminar condensate film flow (c) temperature distribution within the film is linear (d) the vapour space is at constant pressure (e) fluid properties are assumed constant (f) the density of the fluid is much greater than that of the vapour (g) velocity gradients in the circumferential directions are negligible (h) the analysis refers to the upper half of the heat pipe relative to the centre line (i) due to the small taper angle a mean radius is taken for the condenser (j) the condenser wall surface temperature is assumed to be uniform over its length.

Using the above assumptions and the co-ordinate system shown in Fig. 2 a force balance in the x and y direction can be made on the shaded element.

All forces are to be taken per unit periphery the x direction momentum equation Fig. 2(a)

$$\sum Fx = 0 = \frac{\partial \tau}{\partial y} - \frac{\partial \rho}{\partial x} + \rho(\omega^2 r - g)\sin\alpha \qquad (1)$$

the y direction momentum equation Fig. 2(b) neglecting the vapour centrifugal head since $\rho \gg \rho_v$

$$\sum Fy = 0 = -\frac{\partial p}{\partial y} - \rho(\omega^2 r - g)\cos\alpha \qquad (2)$$

the two boundary conditions used in determining the equation for the condensate film velocity distribution are

$$u = 0 \quad \text{at} \quad y = 0$$

and

$$\tau = \mu\frac{\partial u}{\partial y} = -\tau_v\cos\alpha - \frac{dm}{dx}(u_v\cos\alpha + u_\delta) \quad \text{at} \quad y = \delta.$$

Integrating equation (2) between limits y and δ where the pressure is P and P_v yields

$$P = P_v + \rho(\omega^2 r - g)\cos\alpha(\delta - y). \qquad (3)$$

Differentiate (3) with respect to x assuming $dPv/dx = 0$ and substituting in equation (1) gives

$$\frac{\partial \tau}{\partial y} = \frac{\mu\partial^2 u}{\partial y^2} = \rho(\omega^2 r - g)\left\{\cos\alpha\frac{d\delta}{dx} - \sin\alpha\right\}. \qquad (4)$$

This can now be integrated twice to obtain U by applying the above boundary conditions.

$$u = \frac{\rho}{\mu}(\omega^2 r - g)\left(\sin\alpha - \cos\alpha\frac{d\delta}{dx}\right)\left(y\delta - \frac{y^2}{2}\right) - \frac{y\tau_v}{\mu}\cos\alpha - \frac{y}{\mu}\frac{dm}{dx}(u_v\cos\alpha + u_\delta). \qquad (5)$$

When the value of u_v, the vapour velocity is high in comparison with u_δ, the liquid vapour interface velocity, the latter may be neglected, but when they are comparable values then an allowance for u_δ must be made.

The temperature distribution within the condensate film is assumed to be linear. Rohsenow [16] has shown that for Prandtl numbers above one (ordinary fluids) the non-linear distribution of temperature through a thin film due to energy convection is hardly distinguishable. Therefore at any section x at which the film thickness is δ the rate of heat transfer per unit periphery is

$$dQ = k\,dx\frac{(ts-tw)}{\delta} = k\frac{(\theta s)\,dx}{\delta}. \tag{6}$$

Considering the change of phase and assuming that $h_{\bar{f}g}$ is the average enthalpy change of the vapour in condensing to a liquid and sub-cooling to the average liquid temperature of the condensate film.

$$h_{\bar{f}g} = h_{fg} + 0{\cdot}35\,Cp\,\theta s, \quad [16]$$
$$dQ = h_{\bar{f}g}\,dm \tag{7}$$

combining equations (6) and (7) gives the rate of condensation with distance x

$$\frac{dm}{dx} = \frac{k\theta s}{h_{\bar{f}g\delta}}. \tag{8}$$

Eliminating dm/dx from equation (5) and since the slope of the condensate film is assumed to be much less than $\tan\alpha$, $\cos\alpha\,d\delta/dx \ll \sin\alpha$

$$u = \frac{\rho}{\mu}(\omega^2 r - g)\sin\alpha\left(y\delta - \frac{y^2}{2}\right) - y\frac{\tau v\cos\alpha}{\mu} - \frac{k\,\theta s\,Uv\cos\alpha}{\mu h_{\bar{f}g\delta}}y. \tag{9}$$

The mass flow rate of the condensate m can now be determined using

$$m = \int_0^\delta \rho u\,dy.$$

Substituting for u from equation (9)

$$m = \frac{\rho^2(\omega^2 r - q)\sin\alpha\,\delta^3}{\mu}\frac{}{3} - \frac{\rho\tau_v\cos\alpha\,\delta^2}{\mu}\frac{}{2} - \rho\frac{k\theta suv\cos\alpha\,\delta}{\mu h_{\bar{f}g}}\frac{}{2}. \tag{10}$$

Equation (8) can now be integrated remembering the assumption that the film thickness $\delta = 0$ at $x = 0$

$$x = \frac{\rho^2(\omega^2 r - g)\sin\alpha h_{fg}\,\delta^4}{4\mu k\theta s} - \frac{\rho\tau_v h_{fg}\cos\alpha\,\delta^3}{3\mu k\theta s} - \frac{\rho\mu_v\cos\alpha\,\delta^2}{4\mu}. \tag{11}$$

The film thickness distribution along the condenser section is therefore given by

$$Sh_x\left[\frac{\delta}{x}\right]^4 - \tfrac{1}{3}Dr_x\left[\frac{\delta}{x}\right]^3 - \tfrac{1}{4}Rev_x\left[\frac{\delta}{x}\right]^2 - 1 = 0. \tag{12}$$

Where

$$Sh_x = \frac{\rho^2(\omega^2 r - g)\sin\alpha h_{\bar{f}g}x^3}{4\mu k\theta s}$$ Sherwood type number

$$Dr_x = \frac{\rho\tau_v h_{\bar{f}g}x^2\cos\alpha}{\mu k\theta s}$$ friction number

$$Rev_x = \rho\frac{Uvx\cos\alpha}{\mu}$$ two phase Reynolds number

at any section x in the condenser since heat is transferred through the condensate layer by conduction only the local heat flux $Qx = k\theta s/\delta$ and equation (12) can be re-arranged as follows

$$Qx^4 + \tfrac{1}{4}Rev_x\left(\frac{k\theta s}{x}\right)^2 Q_x^2 + \tfrac{1}{3}Dr_x\left(\frac{k\theta s}{x}\right)^3 Qx - Sh_x\left(\frac{k\theta s}{x}\right)^4 = 0. \tag{13}$$

This equation relates the main three parameters controlling the rotating heat pipe operation assuming fixed geometry and a certain working fluid. They are the local heat-transfer flux from the condenser section Qx, the rotational speed ω and the difference between the saturation temperature and the condenser wall temperature $\theta s = (ts - tw)$. The method used to calculate the temperature difference θs when the rotational speed ω and the heat transfer Q are known is shown in Appendix A.

It is possible to develop a similar expression in dimensionless form by defining the average Nusselt number Nu for the condenser section in the following manner

$$Q = h_{\bar{f}g}.m_L. \tag{14}$$

Where m_L is the condensate mass flow rate/unit periphery at $x = L$ and from the definition of the average heat-transfer coefficient

$$Q = h.L.\theta s \text{ (per unit periphery)} \tag{15}$$

$$Nu = \frac{hL}{k} = \frac{h_{\bar{f}g}m_L}{k\theta s}. \tag{16}$$

The condensate flow rate m_L may be obtained from equation (10) which on substitution into (16) gives

$$Nu = \tfrac{4}{3}Sh_L\left(\frac{\delta_L}{L}\right)^3 - \tfrac{1}{2}Dr_L\left(\frac{\delta_L}{L}\right)^2 - \tfrac{1}{2}Rev_L\left(\frac{\delta_L}{L}\right) \tag{17}$$

where suffix L refers to quantities evaluated at the end of the condenser section $x = L$.

It should be emphasised that in all the equations derived so far the Reynolds number Rev has been defined in terms of two phase quantities. The condensate film is assumed to be in laminar motion and the value of the film Reynolds number must be below the transition point. Carpenter and Colburn [17] deduced from experiments with long stationary tubes this transition occurs at film Reynolds number of 240. Cannon and Kays [18] conducted experimental investigations on the effect of tube rotation and found that it had a stabilising influence so that a higher through flow Reynolds number is obtained before transition occurs.

The total volume (charge) of working fluid required for the operation of the rotating heat pipe to transfer a certain heat fluid at a prescribed rotating speed consists of a vapour and liquid phase contribution. The liquid contribution is assumed to be the volume of liquid contained in the condensate film building up along the inner walls of the condenser and adiabatic sections. To calculate the condenser contribution, the heat flux, rotational speed (either assumed or from an experimental run), and heat pipe dimensions must be specified. Equation (13) is solved to obtain the temperature difference θs which is then substituted with the parameters mentioned above into equation (11) to obtain the condensate film distribution along the condenser section. An average value of the film thickness may now be calculated using

$$\delta av = \frac{1}{L}\int_0^L \delta x \, dx$$

and the condenser liquid contribution estimated. The value of the condensate film thickness at exit to the condenser is assumed to be a constant along the adiabatic section and its contribution estimated. In the present analysis the liquid contribution in the evaporator section is assumed to be small enough to be neglected, this will counter balance the over estimate in the adiabatic section. The vapour space in the heat pipe is assumed to be filled with dry saturated vapour at an assumed pressure level corresponding to the heat flux. Knowing the inner volume of the heat pipe enables the vapour contribution to be determined.

A computer programme has been developed for the evaluation of all the results. For a varying geometry heat pipe containing a known working fluid and an input of the fixed parameters Q and ω the computer will print out values of θs, Rev, Nu and δ distribution for the condenser. The programme will also evaluate the required volume of the working fluid charge split in the form of liquid and vapour contribution.

The foregoing analysis can be used to provide information for the initial design of the heat pipe as the computer programme can explore theoretically the effect of varying the geometry of the heat pipe. It is also possible to produce performance trends of the heat pipe operating with different fluids at different heat loads and with varying rotational speeds.

The heat pipe dimensions (taper angle α, length of the condenser section L and the average radius of the condenser section r) have a considerable influence on its performance. Using four rotational speeds Fig. 3 shows that the heat transfer rate increases with taper angle which is a consequence of the increase in the component of centrifugal force ($\omega^2 r \sin\alpha$). The effect of increasing values of the condenser length L also gives higher rates of heat transfer simply because of the increase in heat-transfer area. Increasing the average radius r has a similar effect as it increases both the area and the component of the centrifugal force.

The dimensions used in obtaining theoretical results showing how the different parameters affect the heat pipe operation are those used later during the

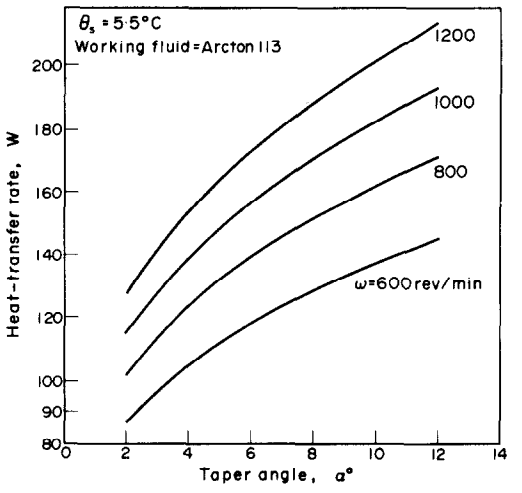

FIG. 3. Effect of taper angle.

experimental phase of the investigation (viz. taper angle 2°, condenser length L = 152 mm, average radius r of the condenser sections 16·9 mm total length of heat pipe 325 mm). The heat transfer rate and rotational speed values are assumed and the working fluid properties are those of ARCTON 113.

The relationship between the heat-transfer rate Q and the temperature difference θs for different rotational speeds "ω" is shown in Fig. 4. These results were

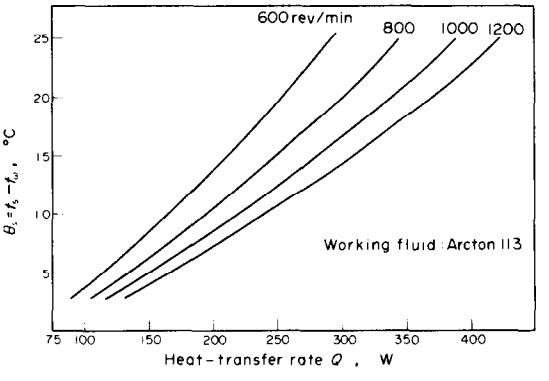

FIG. 4. Theoretical heat-transfer rate Q vs θ_s for different speeds.

obtained by solving equation (13). The graphs show that for a fixed temperature difference θs higher heat-transfer rates are achieved as the rotational speed increases. This is caused by the centrifugal force increasing and hence providing higher condensate flow rates needed for the higher heat pipe performance. A further important fact is that as the centrifugal force increases the thickness of the condensate film decreases thus reducing the thermal resistance and yielding higher heat-transfer coefficients. Figure 5 illustrates the relationship between the two phase Reynolds number Rev and the Nusselt number Nu both evaluated at the end of the condenser section. It is essentially a re-exposition of Fig. 4 in dimensionless form as well as being a graphical interpretation of equation (17). The

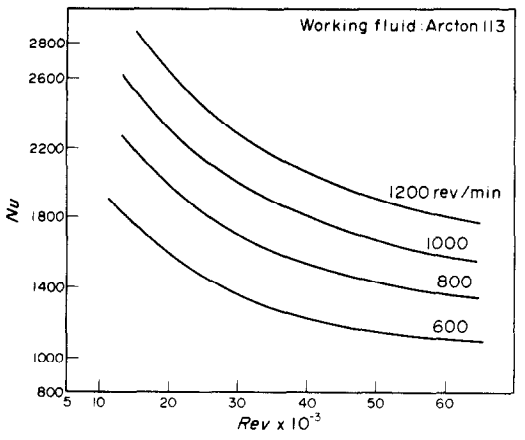

FIG. 5. Theoretical *Rev* vs *Nu* for different rotational speeds.

Reynolds number increases as the vapour velocity increases and since this also has the effect of thickening the condensate layer the Nusselt number decreases for constant rotational speed. However for fixed Reynolds numbers the condensate film thickness decreases as speed increases yielding higher heat-transfer coefficients. The figure also shows that *Nu* approaches zero at very high values of *Rev* where the vapour velocity u_v and the vapour drag are very high, thus causing failure of the heat pipe to transfer any heat.

The effect of the vapour drag forces is shown in Fig. 6. The solid lines represent the case when local friction number *Drx* and Reynolds number *Revx* terms are neglected in equation (13). Although the vapour drag forces increase with heat-transfer rates *Q* Fig. 6 shows that they are important at high heat-transfer rates only. To demonstrate the effect of rotational speed the significance of the vapour drag forces at 300 or 1000 rev/min are shown. The effect of these forces is most significant at the lower speed since the body force (Sherwood number *Sh*) term in equation (13) increases rapidly with increasing "ω" thus cancelling out the effect of the vapour drag terms *Dr* and *Rev*.

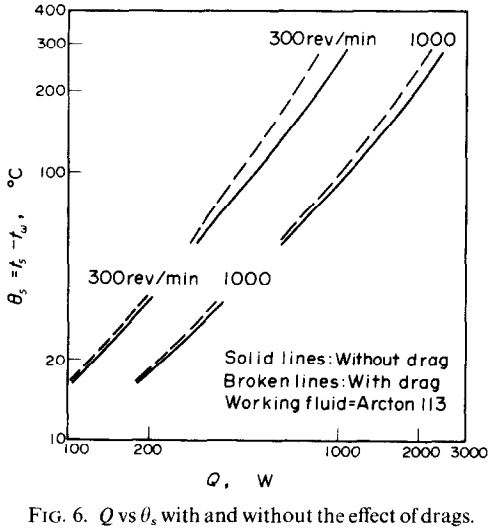

FIG. 6. *Q* vs θ_s with and without the effect of drags.

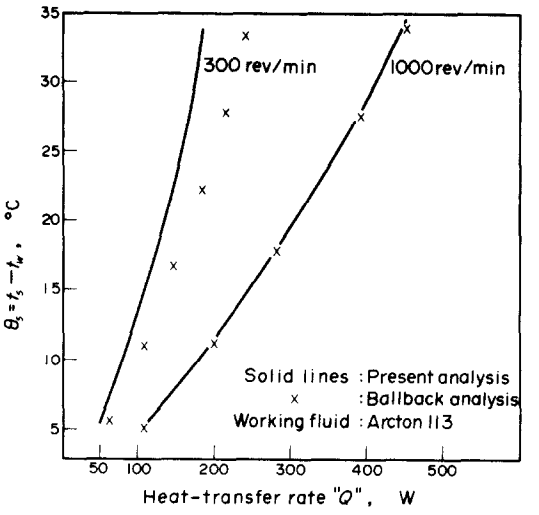

FIG. 7. Comparison of theoretical results with that of Ballback.

Finally Fig. 7 shows a comparison between the present analysis results with those proposed by Ballback [12]. The plot shows that the difference in the analyses increases at the lower rotational speed of 300 rev/min due to the fact that Ballback neglected gravitational effects which become significant at lower speeds.

EXPERIMENTAL APPARATUS AND PROCEDURE

A photograph of the general arrangement of the experimental apparatus is shown in Fig. 8. It consists essentially of the heat pipe, the slip ring assembly for the power supply and thermocouple pick up, the motor drive arrangement, the pressure gauge and safety valve and the power, speed and temperature measuring instruments.

A schematic view of the rotating heat pipe is shown in Fig. 9. The heat pipe is of fixed geometry machined out of solid copper. The overall length was 325 mm the condenser end diameter was 30 mm, whilst the evaporator end was 55 mm. The taper angle used was 2°. It was decided that an evaporator heat input of 2 kW was required and hence a stainless steel sheathed heating cable (Pyrotenax) was wound round the outside of the evaporator section for an evaporator length of 50 mm. This length of heating cable used was estimated to produce a maximum radial heat flux of 83 W/cm^2 equivalent to 7·6 kW. The power was supplied to the heater cable via copper to copper slip rings on the shaft.

In fixing the length of the condenser section it was essential that the condensate film should not become turbulent but remain laminar over its entire length. A low critical liquid film Reynolds' number of 240 was used and resulted in a condenser length of 152 mm for Arcton 113 at a maximum rotational speed of 2000 rev/min for the heat pipe. This was found to be an adequate length for all other working fluids considered.

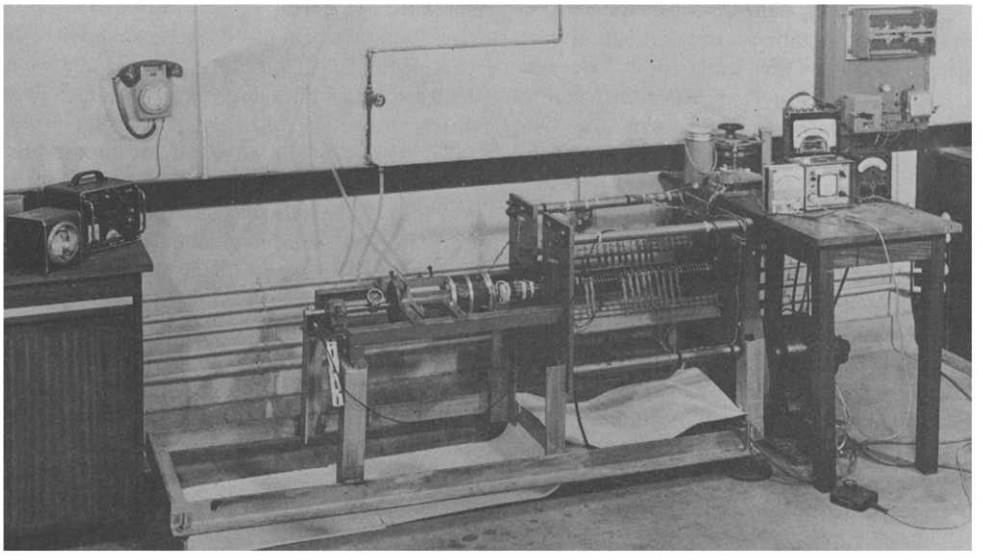

FIG. 8. General arrangement of the experimental apparatus.

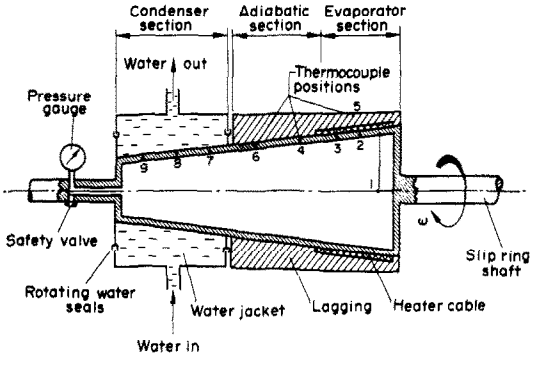

FIG. 9. Schematic view of rotating heat pipe.

The heat sink used for the condenser section consisted of a water jacket which was held stationary. Two "Weston" running seals which were a push fit at both ends of the jacket provided sealing and support for the jacket relative to the rotating heat pipe. Cooling water was supplied to the jacket from a constant head tank. The length of the adiabatic section remaining was 123 mm which was considered to be reasonable in comparison with the evaporator and condenser.

The selection of the suitability of working fluid for the heat pipe can be determined from examining firstly the figure of merit

$$\left(\frac{\rho^2 h_{\bar{f}_g} k^3}{\mu}\right)$$

for the liquid derived in Appendix B, and secondly by considering the fluid's compatability with the heat pipe metal so that corrosion and non-condensable gas generation does not occur. Arcton 113, Arcton 21 and water have low, medium and very high figures of merits respectively and since copper is below hydrogen in the electromotive series the possibility of hydrogen evolution and wall corrosion with these three selected fluids is therefore remote. These three fluids were selected on that basis for the experimental work.

The filling and deaerating procedure for the heat pipe was as follows. The pressure gauge and the safety plug opposite were removed and the heat pipe was evacuated. A known quantity of working fluid (plus a predetermined extra quantity to allow for deaeration) was then drawn into the heat pipe. The exclusion of air from the heat pipe was then ensured by partial evaporation of the charge and bleeding off some of the gas before the heat pipe was sealed and tested for leaks. Arcton 21 fluid was more difficult to use due to its low boiling point 8·9°C. This fluid was forced into the heat pipe under nitrogen pressure before the deaerating procedure.

The features of the thermocouple slip ring units used were basically the same as used by Tarr [19] in his investigation on methods of connection of revolving thermocouples. The temperature distribution along the heat pipe was measured by copper constantan thermocouples placed at positions 1–9, Fig. 9, the outputs of these thermocouples passing along leads through the hollow centred shaft to a series of slip rings. The temperatures were read off in °C directly from a "Cormack" instrument which had a resolution of 0·1°C. The distribution of the thermocouples was as follows: 1, 2 and 3 are in the evaporator section. 1 is placed on the central axis of the heat pipe giving the core vapour temperature. The adiabatic section wall temperature is read by thermocouples 4 and 6, and the condenser wall temperature was given by 7, 8 and 9. The surface temperature of the lagging was measured by 5. The shaft of the condenser had a narrow passage leading to a small pressure gauge which could be observed with the aid of a strobascope. The pressure measurements were not regarded as being accurate but provided a guide to the behaviour of the heat pipe. The true vapour pressure inside the heat pipe was taken as the saturation pressure corresponding to the vapour temperature reading of thermocouple No. 1. There must be a small pressure drop between evaporator and condenser.

The energy balance across the condenser water jacket was required for the estimation of the heat output from the condenser section. The water flow rate was measured by a Rotameter and checked by collecting a certain volume of water and measuring the time required. The total amount of heat transferred to the water in the jacket consists of two parts. The major contribution comes from the heat transferred during the condensation process. A minor contribution comes from the heat generated by friction in the water seals. This heat generation in the seals was predetermined by rotating the heat pipe through its range of speeds without supplying heat to the evaporator, e.g. the heat generated at 300 rev/min was 20 W, and at 1400 rev/min it was 50 W. In analysing the experimental results the heat rate was subtracted from the total amount of heat generated by the condenser jacket water.

The following experimental procedure was carried out to test the foregoing proposed theory. The heat pipe was first filled with the required volume of working fluid. The slip rings and brushes were then thoroughly cleaned with acetone and lubricated with oil containing carbon in suspension. The heat pipe was then rotated at a preselected speed and power was supplied to the evaporator heater. Steady state operating conditions were achieved when the vapour pressure and the various temperature readings stabilized at their respective levels. This usually took 45 min to achieve. Once these steady state conditions were established the thermocouples and vapour pressure were read and the water flow rate from the condenser water jacket was noted to complete the run. The power supplied to the heater was then increased to a predetermined level whilst the rotational speed was kept constant. The same procedure was then followed and repeated for several higher levels of power input until super-heated vapour was generated. This was detected by the rapid increase in the evaporator wall temperature (thermocouple No. 2) indicating a dry wall condition. This condition was accompanied by the rapid divergence between the reading of thermocouple No. 1 measuring the vapour core temperature and the saturation temperature corresponding to the vapour pressure reading recorded. The same procedure was repeated for the different rotational speeds, different fluid charges and different working fluids. To ensure the reproducability of the results some runs were repeated by keeping the power input constant and varying the rotational speed.

Before the heat pipe was charged the inside surface was thoroughly cleaned and degreased using acetone. An inspection of the inside surface was made periodically to ensure that there was no build up of any deposit. This routine was repeated when the working fluid was changed.

EVALUATION OF EXPERIMENTAL RESULTS

The rotating heat pipe was normally operated at four different rotational speeds, 600, 800, 1000 and 1200 rev/min (corresponding to mean centrifugal accelerations of 6·8, 12·1, 18·9 and 27·3 g respectively). For each speed a range of evaporator heat inputs was employed, the maximum heat load input was 1600 W (equivalent to a heat flux of 20 W/cm^2). Three different working fluids, Arcton 113, Arcton 21 and water were used with different charges as a further independent variable.

Theory indicated the paramount importance of the minimum fluid charge required in the operation of the heat pipe. The effect of exceeding this minimum quantity by a significant amount is discussed later. It is therefore necessary to explain how the two phases of this quantity are assessed both experimentally and theoretically. When heat is applied to the evaporator of a charged heat pipe the liquid evaporates and a certain level of vapour pressure is established at steady state conditions. A proportion of the fluid will exist as a liquid the remainder as a vapour which is assumed to be dry saturated. This assumption enables an estimation of the vapour phase contribution to the total volume of the measured fluid charge in the heat pipe to be made. The theoretical fluid charge however can only be calculated by first determining the liquid film thickness contribution on the walls of the condenser and adiabatic sections. This is then added to the vapour contribution which exists at the particular saturation pressure achieved in an experimental run. Theory indicates that the liquid phase contribution increases with increasing heat flux in order that the higher heat-transfer rates can be promoted, and therefore this quantity will vary even with constant rotational speed. The main outcome of this is that while it is only practical to use a constant charge of working fluid in a series of experimental runs, theoretically the indication is that the charge should be varied. This factor will be discussed later when it is seen to have a critical effect on the empirical results obtained.

The major proportion of the experimental programme used Arcton 113 as a working fluid. Theory predicted that 12 cm^3 represented a high level of total charge of Arcton 113 and 6 cm^3 was a low level, tests were thus conducted using 12, 8 and 6 cm^3 respectively. The charges of Arcton 21 and water were determined in a similar manner yielding values less than those for Arcton 113 due to their higher values of "h_{fg}".

Tests were conducted with 30 cm^3 charge of Arcton 113 to determine the effect of over filling. The experimental results disagreed with the theoretical prediction. Increasing the rotational speed of the heat pipe had a negligible effect on the heat transfer Q in the condenser and the experimental results of θs vs Q (similar to those shown in Figs. 11 and 12) for a speed range 600–1400 rev/min all lay on a very narrow band. From the subsequent experience of operating the heat pipe with lower charges such as 12 cm^3 it becomes obvious that the required heat input to the evaporator has to produce a slight superheat in the vapour. For the 30 cm^3 charge it was impossible to supply this heat through the slip ring heater cable arrangement of the present apparatus. Theory and experiment agreed when the liquid film of the evaporator was being completely vapourised producing a slightly superheated vapour core.

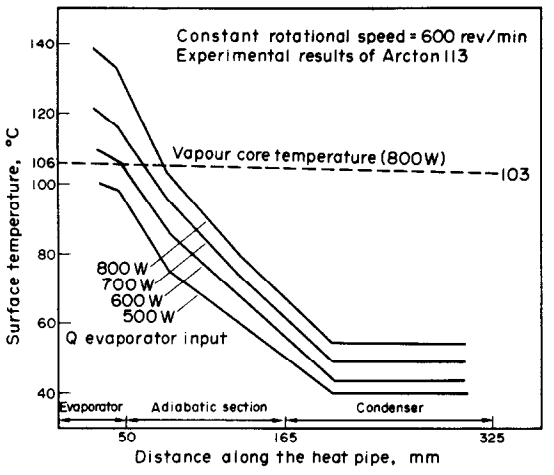

FIG. 10. Typical surface temperature distribution along the heat pipe (constant rotational speed).

A typical surface temperature distribution of the wall of the heat pipe is shown in Fig. 10 for different evaporator heat input levels at a constant speed of rotation 600 rev/min for 12 cm^3 charge Arcton 113. There is a substantial temperature drop in the axial direction between evaporator and condenser. This temperature drop is very high when compared with that experienced with conventional heat pipes. This may well be due to a high temperature drop between the vapour core in the heat pipe and the condensate liquid film surface. The outside condenser wall surface is purposely being kept low by the coolant flow thus producing a comparatively cold sink. The vapour temperature distribution for the 800 W case is shown as a dotted line. This is the temperature drop as recorded by thermocouple No. 1 on the centre line in the evaporator and the saturated temperature in the condenser estimated from the pressure gauge reading taken at that point. This is not regarded as being very accurate but the pressure gauge readings were such that the corresponding *ts* values were 3–5°C consistently lower than thermocouple No. 1 for steady state conditions of operation.

Figures 11 and 12 show the relationship between the condenser heat-transfer rate Q and the temperature difference θs (where θs is the difference between saturation temperature *ts* and condenser wall temperature *tw*) for different rotational speeds and working fluid charges. For each graph the theoretical values of the temperature differences are obtained as follows. Measured values of the heat transferred from the condenser section Q, rotational speeds ω, heat pipe dimensions, and the properties of the working fluid of the saturation temperature prevailing in the system are all fed into the computer programme. Thus equation (13) is solved and yields the corresponding theoretical values of the temperature difference θs. The experimental values of θs were obtained from *ts* read by thermocouple No. 1 and *tw* and the average of thermocouple readings No. 7, 8 and 9. Figure 11 shows that for a working fluid charge of 12 cm^3 experimental and

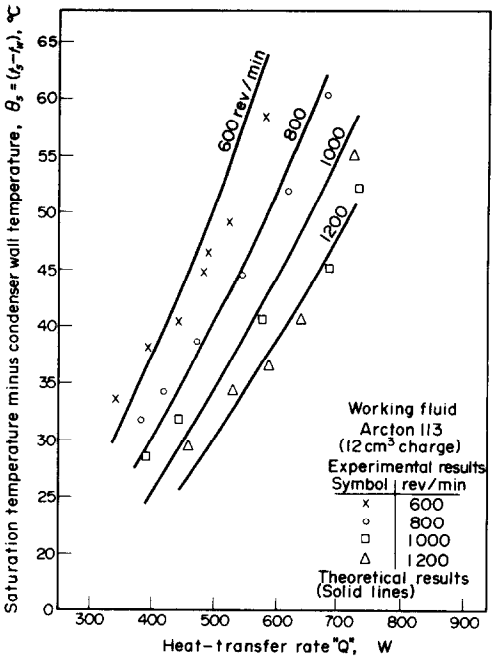

FIG. 11. θ_s vs heat transfer Q for different rotational speeds (Arcton 113, 12 cm^3).

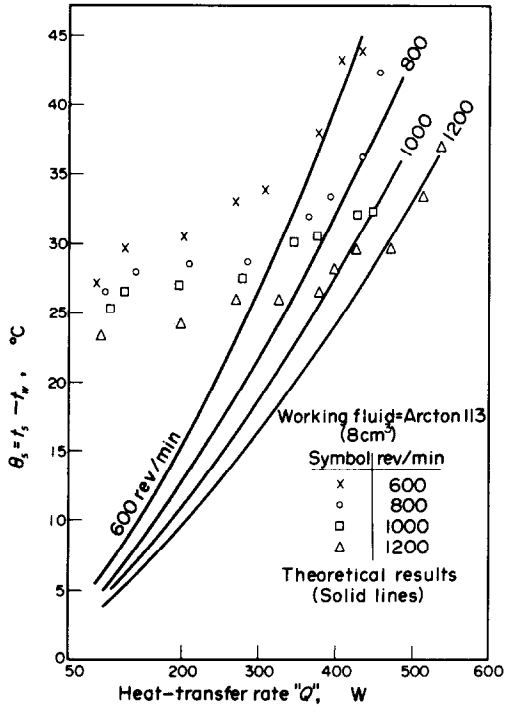

FIG. 12. θ_s vs heat-transfer rate Q (Arcton 113, 8 cm^3).

theoretical data are in general agreement. When θs is constant increasing the rotational speed produces increases in the centrifugal forces and consequently higher condensate flow rates resulting in larger heat-transfer rates. Increases in the centrifugal force decreases the condensate film thickness which in turn yields higher heat-transfer coefficients and hence lower temperature differences for a fixed heat-transfer rate.

When a working fluid charge of 8 cm^3 was investigated a similar behaviour in the experimental results was observed. However in this case greater deviations occurred between the experimental data and the theoretical curve. An explanation for this is assumed to be that the theoretical analysis predicts a minimum fluid charge directly related to the heat transfer Q and the rotational speed ω. Therefore for all the lower ranges of heat transfer Q the theoretical quantity of fluid charge required within the system was much less than the 8 cm^2 experimental charge. All the experimental results to the left of the theoretical curves are those related to an excess of liquid trapped within the system. The vapour produced is likely to be wet and the condensate film thickness is likely to be excessive causing a higher value of θs than predicted theoretically due to the increased thermal resistance of the condensate film. For a charge that is slightly less than the theoretical value a small degree of superheating may ensue without breakdown of the two phase system. Good agreement occurs between experimental and theoretical results for both the 12 and 8 cm^3 charges when theory predicted the charge to be 12 and 8 cm^3 respectively and when slight superheat was observed in the experimental readings. When the low level charge of 6 cm^3 was used the experimental θs values were far higher than the theoretically predicted values over the entire range, thus indicating very low heat-transfer coefficients. Though the 6 cm^3 fluid charge was predicted theoretically at some points in the theoretical curves the failure to produce compatible results can only be explained by the inability of the small fluid charge to completely wet the condensing and evaporating surfaces, which is essential for the two-phase heat transfer cycle to operate satisfactorily. Similar trends to this were observed when water was used on the working fluid and will be discussed later.

Examination of the experimental results Figs. 11 and 12 shows that the rate of increase of heat transfer with rotational speed tends to fall off as the higher speed ranges are approached. This suggests that there is an upper envelope for lines of constant speed above which no increase in heat transfer occurs with increase in speed. The following physical explanation of this can be made. Theoretically the liquid condensate film decreases with increase in rotational speed. Assuming that the level of resistance to the flow of condensation is influenced by the surface finish of the wall it will therefore disturb the thinner layers rather than the thicker layers. Consequently insufficient circulation of the condensate might be induced for the adequate removal of heat. Morris [20] carried out experimental and theoretical work on a rotating single phase thermosyphon and observed similar trends in the heat-transfer characteristics which he attributed to the increase in resistance to flow caused by the speed of rotation.

Some of the foregoing results are plotted non-dimensionally as Nusselt numbers Nu vs two phase Reynolds number Rev see Fig. 13. The Nusselt number is seen to be nearly constant with the theoretical curves passing through the midst of the points of any particular

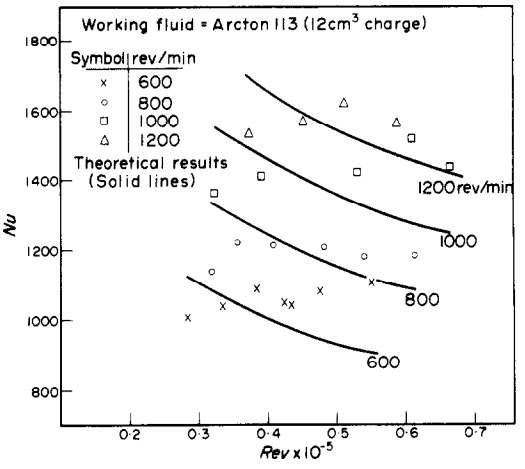

FIG. 13. Nu vs Rev for Arcton 113 (12 cm^3 charge).

speed run. Again the agreement depends on the compatability of the working fluid charge in the experiments with the theoretical values.

Besides Arcton 113, Arcton 21 and water were used to investigate the effect of working fluid properties on the heat pipe performance. In this respect the parameter under examination is the fluid property group defined by

$$\left(\frac{\rho^2 h_{\bar{f}_g} k^3}{\mu}\right) \text{liquid}.$$

The property group for water was 2000 times greater than Arcton 113 whilst that of Arcton 21 was only 5 times as great. In view of this the performance of the heat pipe using water should be superior to those of the other two fluids with Arcton 21 being better than the 113 fluid.

The results for the Arcton 21 substantiated this improvement whilst remaining similar in form to the Arcton 113 results.

The experimental results using water as the working fluid were not as expected. The maximum fluid charge that was calculated for the experiments based on a maximum evaporated heat input of 1·8 kW was found to be 5 cm^3, a relatively low value which was a consequence of the very high fluid property value. For all runs using this charge no agreement was achieved between the empirical or theoretical data. As a typical example at a rotational speed of 800 rev/min and condenser heat-transfer rate of 540 W the observed temperature difference θs between condenser wall and saturation value was 80°C whilst that predicted theoretically was of the order of 3°C.

The experimental data for water was similar to that obtained in tests performed utilizing the 6 cm^3 charge of Arcton 113 and the reason for the difference between theory and experiment must be the case. There is insufficient water fluid to establish a stable evaporation and film condensation cycle. A further feature of the heat pipe operating in this condition was that more heat was conducted axially through the adiabatic section, in some cases it was calculated to be as much as double that in the Arcton 113 runs. The experimental

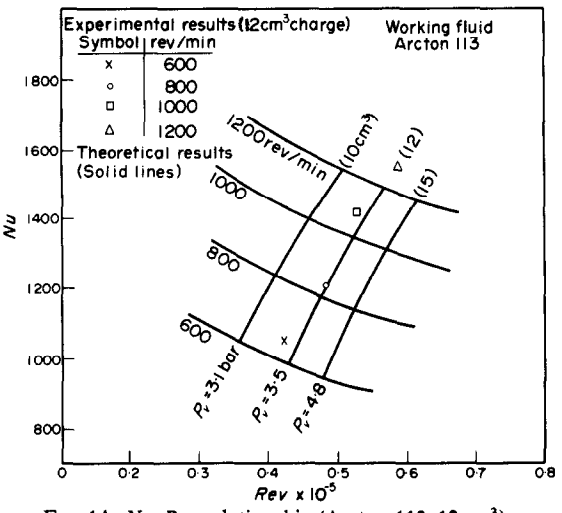

FIG. 14. *Nu–Rev* relationship (Arcton 113, 12 cm³).

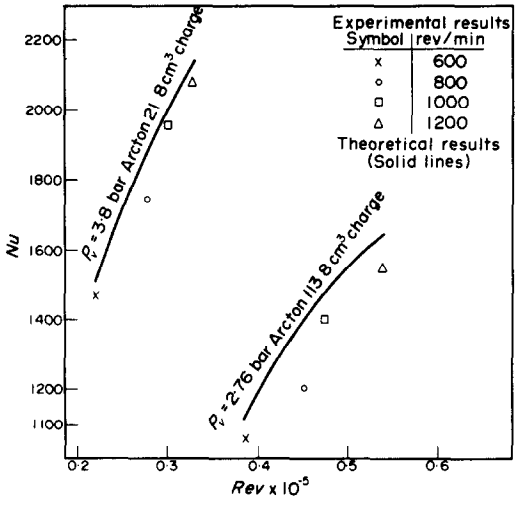

FIG. 15. *Nu* vs *Rev* relationship for different working fluids.

performance of the rotating heat pipe using water as a working fluid cannot be assessed using the present apparatus because of the small fluid charge used. It was not possible to increase the charge substantially due to the inability of the evaporator heater to provide the necessary heat fluxes.

For the optimum operation of the heat pipe with stable two phase transfer cycle there is a unique working fluid charge for a particular set of conditions (i.e. heat flux and rotational speed). Theoretical curves of Nusselt number *Nu* vs Reynolds number *Rev* can be drawn. Superimposed on the curves are marked lines which link points of constant fluid charge, e.g. in Fig. 14 fluid charge lines for 10, 12 and 15 cm³ are shown. From the experimental results for the 12 cm³ charge the values of the *Rev* nearest to those of the theoretical points are plotted and show good agreement. The effect of the fluid property group is illustrated in Fig. 15 for Arcton 21 and 113. Lines of constant charge of 8 cm³ have been extracted from *Nu–Rev* theoretical curves with experimental points marked in. Again there is good agreement and also the superior heat-transfer properties of Arcton 21 over Arcton 113 is clearly demonstrated.

CONCLUSIONS

From the theoretical and experimental investigations carried out the following conclusions can be made.

The rotating heat pipe which utilizes the vapourization condensation cycle is a feasible system for transferring heat efficiently. Its equivalent conductivity when compared with a copper rod of similar geometry was several hundred times higher.

The rotating heat pipe performance may be predicted using a Nusselt type analysis applied to the condenser section which relates the heat-transfer rate, rotational speed, working fluid properties and geometry. The analysis enabled the prediction of the effect of vapour drags which was found significant only at high heat fluxes. It was also possible to examine the influence of the heat pipe geometry on the performance and it was found that increasing the length of the condenser, taper angle or average radii improved the heat transfer. The fixed geometry heat pipe tested was designed for moderate heat fluxes lower than the boiling limit values. The entrainment and sonic limits familiar to stationary heat pipes were not attained since the extremely high vapour velocity required can only be obtained using very high heat fluxes. Vapour drags were not significant due to the same reason.

The agreement between experimental and theoretical results depends upon the following three conditions (a) compatability of the working fluid charge existing in the apparatus with that predicted theoretically; (b) the existence of sufficient fluid charge to provide surface wettability and hence establish a vapourization–condensation cycle; and (c) the heat-transfer rate should be suitable to provide vapour at near dry saturated conditions.

The rotation of speed enhances the heat transferring capability of the heat pipe due to the decrease in thermal resistance of the condensate film brought about by the reduction in its thickness. However over the speed range employed it appears that the rate of increase of heat transfer with speed tends to decline thus indicating an upper speed limit.

It was demonstrated theoretically that fluids with higher values of the "property group" should be more effective for the heat pipe operation and therefore both water and the Arcton 21 should be superior to Arcton 113. In the experiments conducted and as predicted Arcton 21 yielded higher Nusselt number values than Arcton 113 but in the case of water this was not so. The reason is believed to be the insufficient water charge for establishing a vapourization–condensation cycle. Higher fluid charges were not possible due to the inability of the present heating element to provide higher heat fluxes.

Practical applications of the rotating heat pipe have already been reported in two recently published papers by Polasek [21] and Groll *et al.* [22]. Polasek has conducted experimental work on cooling the shaft of an AC motor using a heat pipe configuration and found that the temperature of the rotor and stator windings was considerably reduced. The machine output could then be increased by 15 per cent. Groll *et al.* reported

utilizing the rotating heat pipe principles for temperature flattening of rotating drum surfaces. Plastic wires and fibres are stretched on hot rotating drums whose surface was kept isothermally at 250°C rotating at 4000–6000 rev/min. In the future there will undoubtedly be many further new applications of this relatively simple device.

Acknowledgements—The authors wish to express their gratitude to Professor F. T. Barwell who gave them advice and encouragement when carrying out the work described in this paper.

REFERENCES

1. R. S. Gaugler, Heat pipe, U.S. Patent 2350348 (8 January 1944).
2. G. M. Grover *et al.*, Structures of very high thermal conductance, *J. Appl. Phys.* **35**, 1990 (1964).
3. International Heat Pipe Conference, Institut fur Kernenergetik (IKE), University of Stuttgart (1973).
4. A. A. G. Asselman and D. B. Green, Heat pipes, *Phillips Tech Rev.* **33**(4), 104–113, (5) 138–148 (1973).
5. D. Chisholm, The heat pipe, M & B Tech LIB TL/ME/2 (1971).
6. Analysis, design and manufacture of heat pipes, N.E.L. (June 1973).
7. V. H. Gray, The rotating heat pipe, ASME Paper No. 69-HT-19 (1969).
8. V. H. Gray, P. J. Mario and A. W. Joslyn, Boiling heat transfer coefficients; interface behaviour and vapour quality in rotating boiler operating up to 475 *G's*, NASA TN D 4136 (March 1968).
9. C. P. Costello and J. M. Adams, Burn out heat fluxes in pool boiling at high accelerations, Mech. Eng. Dept., University Washington (1960).
10. E. M. Sparrow and J. P. Hartnett, Condensation on a rotating cone, *J. Heat Transfer* **83C**(1), 101–102 (1961).
11. P. J. Mario, T. J. Daley and L. J. Ballback, An analytical and experimental investigation of rotating non-capillary heat pipes, Annual Report NPS-59 MX 70061 A Monterey Calif. U.S. Naval Postgraduate School (AD 709907) (1970).
12. L. J. Ballback, The operation of a rotating wickless heat pipe, M.Sc. Thesis Monterey Calif. U.S. Naval Postgraduate School (AD 701674) (1969).
13. T. J. Daley, The experimental design and operation of a rotating wickless heat pipe, M.Sc. Thesis Monterey Calif. U.S. Naval Postgraduate School (AD 709923) (1970).
14. W. Nusselt, Die Oberflaechenkondensation des Wasser-Dampfes, *Z. Ver. Dt. Ing.* **60**, 541 (1916).
15. Y. R. Mayhew, D. J. Griffiths and J. W. Phillips, Effect of vapour drag on laminar film condensation on a vertical surface, *Proc. Inst. Mech. Engrs* **180**(3J), 280–287 (1965–1966).
16. W. M. Rohsenow, Heat transfer and temperature distribution in laminar film condensation, *Trans. Am. Soc. Mech. Engrs* **78**, 1645–1648 (November 1956).
17. E. F. Carpenter and A. P. Colburn, The effect of vapour velocity on condensation inside tubes, Proc. General Discussion on Heat Transfer, London (Inst. Mech. Engrs., London) (11–13 September 1951).
18. J. N. Cannon and W. M. Kays, Heat transfer to a fluid flowing inside a pipe rotating about its longitudinal axis, *J. Heat Transfer* **91C**, 135–139 (February 1969).
19. P. R. Tarr, Methods for connection to revolving thermocouples, Lewis Flight Propulsion Lab. Cleveland Ohio, NACA RM E50 J23a (January 1951).
20. W. D. Morris, Heat transfer characteristics of a rotating thermosyphon, Ph.D. Thesis Univ. College of Swansea (Wales) (1964).
21. F. Polasek, O. Oslejsek and M. Bubenicek, Chlazeni rotoru elektromotoru valcovou rotacni tepelnou, *Elektrotechn. Obz.* **63**(1), 40–46 (1974).
22. M. Groll, W. D. Munzel, H. Kreeb and P. Zimmermann, Industrial applications of low temperature heat pipes, Proceedings of International Heat Pipe Conference, IKE-VDI, Stuttgart (October 1973).
23. C.-F.-Chen and I. John Haas, *Elements of Control System Analysis.* Prentice Hall, Englewood Cliffs (1968).

APPENDIX A

Method used to Calculate the Temperature Difference θ_s when the Rotational Speed ω and the Heat-Transfer Rate Q are known

The method used to solve equation (13) when ω, and Q, heat pipe dimensions, and working fluid properties are known is summarized as follows.

Equation (13) $$Qx^4+\tfrac{1}{4}Re v_x\left[\frac{k\theta s}{x}\right]^2 Qx^2 + \tfrac{1}{3}Dr_x\left[\frac{k\theta s}{x}\right]^3 Qx - Sh_x\left[\frac{k\theta s}{x}\right]^4 = 0.$$

(a) Neglect the drag terms, i.e. the second and third terms

$$Qx^4 = Sh_x\left[\frac{k\theta s}{x}\right]^4$$

an expression for the average heat-transfer rate may be obtained by using

$$Q = \frac{1}{L}\int_0^L Qx\,dx = \tfrac{4}{5}Q_L$$

(b) Substitute $Q = \frac{4}{5}Q_L$ to obtain an equation which relates Q, ω, and θs.

(c) Substitute the known values of Q and ω and solve for θs.

(d) From the known Q value calculate the vapour velocity u_v and the vapour shear stress as follows

$$Q = \dot{m}_v h_{fg} \quad \dot{m} = \rho_v u_v A_c \quad \text{hence} \quad u_v.$$

This value of the vapour velocity u_v should be multiplied by $\cos\alpha$ due to the tapered condenser wall

$$\tau_r = \tfrac{1}{2} f . \rho_v . u_v^2 \quad \text{where } f \text{ is the friction factor.}$$

If vapour flow is laminar $Red < 2000$ $f = \dfrac{16}{Red}$

If vapour flow is turbulent $Red > 2000$ $f = \dfrac{0{\cdot}0791}{(Red)^{0{\cdot}25}}$

where $Red = \dfrac{\rho_v u_v A_c}{\mu_v}$

$A_c = \pi r^2$ (r = radius at entrance to the condenser).

Since u_v is multiplied by $\cos\alpha$ therefore τ_r is implicitly multiplied by $\cos\alpha$ when the vapour flow is laminar and by $(\cos\alpha)^{1{\cdot}75}$ when the flow is turbulent.

(e) Substitute θs and u_v, t_v into equation (13) in its complete form. This results in an equation relating the local heat-transfer flux Qx to the distance along the condenser section x.

(f) The equation obtained from step (e) relating Qx to x may now be solved using Newton–Raphson method quoted in [23] and applying Simpson's rule an average value of Q is obtained.

(g) The average value Q obtained from (f) is compared with the initially known Q value. One of the following situations is now possible.

(i) If the difference between the two Q values is within the required accuracy, the temperature difference θs value from step (c) is a correct solution for the particular set of values of Q, ω, dimensions and fluid properties.

(ii) If the difference between the two Q values is not within the acceptable limits then θs from step (c) is not a correct solution and one of the following steps should be taken.

(iii) If the calculated value of Q is higher then the known value θs from step (c) is too high. A new value of θs which is lower than before is therefore assumed and the procedure is repeated starting from step (e).
(iv) If the calculated value of Q is lower then the opposite of (iii) above is executed.

APPENDIX B

Derivation of the Property Group

A dimensional property group which determines the figure of merit of a working fluid may be derived from the theoretical analysis as follows.

From Appendix A

$$Qx^4 = Sh_x\left[\frac{k\theta s}{x}\right]^4 \quad \text{and} \quad Q = \tfrac{4}{3}Q_L$$

these combine to give

$$Q^4 = Sh_L\left[\frac{k\theta s}{0{\cdot}75L}\right]^4$$

from equation (12)

$$Sh_L = \frac{\rho^2(\omega^2 r - g)\sin\alpha\, h_{\bar{f}g} L^3}{4\mu k\theta s}.$$

hence

$$Q^4 = \frac{(\omega^2 r - g)\sin\alpha\,\theta s^3}{(1{\cdot}26)L}\left[\frac{\rho^2 h_{\bar{f}g} k^3}{\mu}\right].$$

Therefore the property group is

$$\left[\frac{\rho^2 h_{\bar{f}g} k^3}{\mu}\right].$$

ETUDE DES FACTEURS QUI AFFECTENT LE FONCTIONNEMENT D'UN TUBE ECHANGEUR ROTATIF

Résumé—Le tube échangeur rotatif est un dispositif qui utilise un cycle thermique à deux phases. La rotation autour de l'axe longitudinal engendre un champ de force centrifuge dont une composante agissant le long des parois effilées aspire le condensat vers l'évaporateur.

Une analyse théorique du type de celle de Nusselt est proposée pour le film condensé, elle tient compte des effets de trainée dans la vapeur circulant en sens inverse. Une prévision du fonctionnement permet de relier entre eux, les taux de transfert thermique, vitesses de rotation, différences de température à travers les films condensés, propriétés du fluide et géométrie du tube.

L'étude expérimentale permet de tester l'analyse et fournit un bon accord pour les deux Arcton 113 et 21 fluides mais aucun accord n'est obtenu pour l'eau. Une explication de ce fait est proposée.

UNTERSUCHUNG DER FAKTOREN, DIE DIE LEISTUNG EINES ROTIERENDEN HEIZROHRES BEEINFLUSSEN

Zusammenfassung—Das rotierende Heizrohr arbeitet mit einem Zwei-Phasen-Kreislauf für die Wärmeübertragung. Die Rotation um die Längsachse erzeugt ein zentrifugales Kräftefeld mit einer Komponente, die entlang der konischen Wand wirkt und das Kondensat zum Verdampfer zurückbringt.

Für die Untersuchung des Kondensatfilms wird ein Ansatz nach Nusselt vorgeschlagen, wobei die mitreißende Wirkung des in Gegenrichtung strömenden Dampfes berücksichtigt wird. Eine theoretische Beziehung für die Leistung korreliert Wärmeübertragungsverhältnisse, Drehgeschwindigkeit, Temperaturdifferenzen quer zum Kondensatfilm, Stoffwerte und Geometrie des Heizrohres.

Eine experimentelle Auswertung der Untersuchung zeigt gute Übereinstimmung für die Stoffe Arcton 113 und 21, aber keine Übereinstimmung für Wasser. Eine Erklärung dafür wird vorgelegt.

ИССЛЕДОВАНИЕ ФАКТОРОВ, ВЛИЯЮЩИХ НА РЕЖИМ РАБОТЫ ВРАЩАЮЩЕЙСЯ ТЕПЛОВОЙ ТРУБКИ

Аннотация — Вращающаяся тепловая трубка представляет собой устройство с двухфазным циклом теплопереноса. Вращение по продольной оси образует поле центробежных сил, а составляющая этих сил, действующая вдоль конической стенки, нагнетает конденсат назад в испаритель.

Предлагается теоретический анализ типа Нуссельта для пленки конденсата с учетом силы торможения обратного течения пара.

Определение режима работы связывает скорости теплопереноса, скорости вращения, разности температур по толщине пленки конденсата, свойствами жидкости и геометрией тепловой трубки.

Проведенные опыты на двух жидкостях (Арктон 113 и 21) дали хорошее согласие с теорией. Исключение составили опыты с водой. Приводится объяснение этого несоответствия.